SAND2021-11767C

Scoping and concept design of a WEC for autonomous power

Umesh A. Korde
Dept. of Environmental Health and Engineering
Johns Hopkins University
Baltimore, MD, USA
ORCID: 0000-0002-0103-7353

L. Andrew Gish
Dept. of Naval Architecture and Ocean Engineering
United States Naval Academy
Annapolis, MD, US
ORCID: 0000-0003-0807-9609

Giorgio Bacelli
Water Power Technologies Department
Sandia National Laboratories
Albuquerque, NM, USA
ORCID: 0000-0002-1208-2352

Ryan G. Coe
Water Power Technologies Department
Sandia National Laboratories
Albuquerque, NM, USA
ORCID: 0000-0003-0738-3772

***Abstract*— This paper reports results from an ongoing investigation on potential ways to utilize small wave energy devices that can be transported in, and deployed from, torpedo tubes. The devices are designed to perform designated ocean measurement operations and thus need to convert enough energy to power on-board sensors, while storing any excess energy to support vehicle recharging operations. Examined in this paper is a traditional tubular oscillating water column device, and particular interest here is in designs that lead to optimization of power converted from shorter wind sea waves. A two step design procedure is investigated here, wherein a more approximate two-degree-of-freedom model is first used to identify relative dimensions (of device elements) that optimize power conversion from relative oscillations between the device elements. A more rigorous mathematical model based on the hydrodynamics of oscillating pressure distributions within solid oscillators is then used to provide the hydrodynamic coefficients, forces, and flow rates for the device. These results provide a quick but rigorous way to estimate the energy conversion performance of the device in various wave climates, while enabling more accurate design of the power take-off and energy storage systems.**

***Index Terms*—wave energy converter (WEC), autonomous underwater vehicle (AUV), blue economy, self-powered sensor platforms.**

I. Introduction

Wave energy converter (WEC) design has traditionally targeted large scale devices for grid generation. However, more recently there is increasing interest in designing wave energy devices for alternative applications. These so-called "blue economy" devices may consider power sensors for oceanography research, supporting an aquaculture farm, generating pressure for a water desalination plant, or recharging autonomous underwater vehicles (AUV) [1], [2].

Green et al. [2] looked generally at blue economy needs, providing a characterization of power demands and other design constraints based on surveys of potential users. This study reported that AUVs required, on average, 200 W of power. Most sensor systems were reported to require less than 20 W of power. Driscoll et al. [3] performed a scaling and scoping study to assess the potential for WECs to support AUV recharging.

Several potential users in the Defense and Ocean Science/Technology communities were surveyed at the start of this research. Survey results seem to suggest two perspectives: (1) a wave-power/oceanographic developers perspective, and (2) a Defense-Systems engineers perspective. With (1), power maximization and long-term, reliable, uninterrupted instrument support are a priority, while with (2), power conversion with minimal parasitic consumption, high flexibility with stowage and deployment options, low-cost, and above all, covert operation seem crucial. Both perspectives present interesting challenges and solution possibilities that could be worth exploring further. Our current goal is to investigate design choices primarily geared toward military applications.

This paper discusses our ongoing work on small, torpedo-tube deployable free-floating devices that operate below the surface, and are designed to convert enough power to keep an on-board battery charged and to power a limited set of sensors along with limited bandwidth communications at random intervals. Presented in this paper are, (i) steps leading to our broader design decisions, (ii) principal results from our mathematical modeling work undertaken to gain useful insights into the impact of geometry on performance.

The power conversion technique being pursued here is one of the five design options examined early in this research, and was chosen in part because the mechanical components are not

Sandia National Laboratories is a multi-mission laboratory managed and operated by National Technology and Engineering Solutions of Sandia, LLC., a wholly owned subsidiary of Honeywell International, Inc., for the U.S. Department of Energy's National Nuclear Security Administration under contract DE-NA0003525. U.A. Korde would like to thank Sandia National laboratories and the Department of Energy for their support. This paper describes objective technical results and analysis. Any subjective views or opinions that might be expressed in the paper do not necessarily represent the views of the U.S. Department of Energy or the United States Government.

normally in direct contact with water, and because the system is capable of long-term unattended, free-floating operation without the need for frequent retrievals and maintenance. The basic concept of tail-tube oscillating water column buoys has received attention since the mid-1970's, and dates back even further to the early work of Masuda [4]. Oscillating water columns inside floating buoys were also analyzed and tested by Budal and Falnes [5] and Whittaker [6]. Examples of hydrodynamic analysis include [7]. More recent work includes the models used by Falcao and coworkers (particularly [8] and [9], etc.).

II. Hydrodynamic Modeling

Figure 1 shows a schematic view of the device being modeled here. Small-amplitude waves and small-amplitude motions are assumed. The hydrodynamically more accurate model treats a coupled system wherein the oscillating pressure inside the OWC chamber interacts with the surrounding wave field and the moving hull of the tube with the flotation collar. This treatment is based on the formulation of Evans [10] as extended by Falnes and McIver [11] to oscillating water columns within floating bodies. The more approximate model treats the water inside the tube hull as a quasi-rigid body whose oscillations are dynamically coupled to the oscillations of the tube that contains it. The expectation, to be tested in this work, is that the tube and water column diameters are small enough (relative to realistic wave lengths) for the water plane inside the tube to rise and fall uniformly. The model based on the quasi-rigid body approximation is described first, and is used initially to help in the design of the test models.

A. Coupled Model with Rigid-Body Approximation

This analysis technique is first used to estimate the two natural frequencies of the two-degree-of-freedom system formed by the float and the quasi-rigid body oscillating water column. This analysis can thus readily be used for design purposes. Heave oscillation is assumed to dominate. Assuming that the tube with the oscillating water column is small in diameter relative to the wavelengths of interest, the oscillating water column is modeled as a single heaving body with rest-mass equal to the mass of the water in the tube. Its oscillation is coupled to that of the buoy via stiffness, as water displaced by its oscillation causes a force on the buoy and vice versa.

In the present work, this model is used for geometry design and for estimation of the two coupled natural frequencies of the device in heave. Letting M_1 denote the sum of in-air mass and infinite-frequency added mass for the collar + the small mass of the tube structure, with M_2 representing the equivalent quantity for the water in the tube,

$$M_1 = \rho A_{wp} D_r + \overline{a}(\infty); \quad \text{and } M_2 = \rho a_{wp} \ell (1 + \ell_\infty). \quad (1)$$

The tube thickness is assumed to be small and its mass is neglected in this analysis. The stiffness constants for the two masses are,

$$k_1 = \rho g A_{wp}, \quad \text{and } k_2 = \rho g a_{wp}. \quad (2)$$

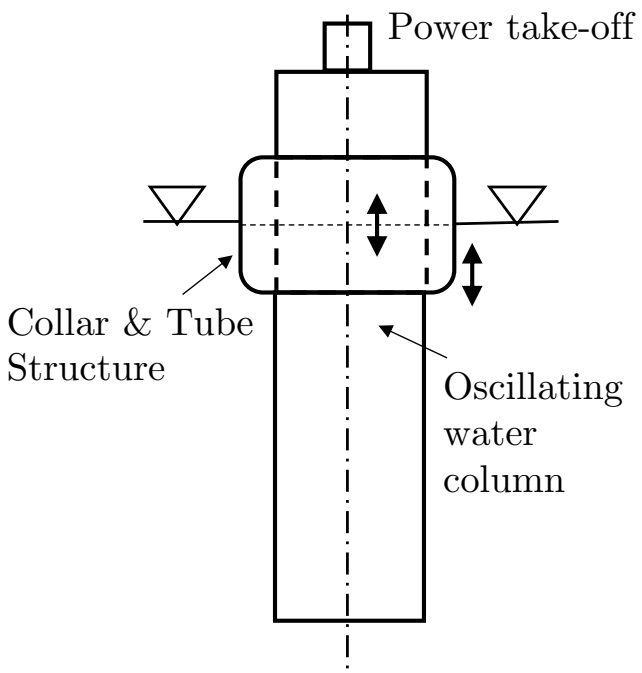

Fig. 1: Schematic view of the torpedo-tube deployable device with a collar and an oscillating water column.

Here, D_r denotes the draft at which the collar structure floats, $\overline{a}(\infty)$ denotes the infinite-frequency added mass for the collar+tube structure, while ℓ and ℓ_∞ denote the length and infinite-frequency added-length of the water in the tube. Since the interest here is in using this approximation to predict the approximate natural response of the system, damping effects are ignored. For the same reason, exciting forces, radiation forces (including frequency-dependent radiation damping and frequency-dependent added mass) also do not need to be included in the present model.

With the help of free-body and kinetic diagrams, the equations of motion for the two-degree of freedom system here can be written as,

$$\begin{aligned} M_1 \ddot{x}_1 &= -k_1 x_1 - k_2 (x_1 - x_2), \\ M_2 \ddot{x}_2 &= k_2 (x_1 - x_2). \end{aligned} \quad (3)$$

These equations can easily be rewritten in matrix form. Along the way, letting

$$x_1 = X_1 \mathrm{e}^{i\Omega t}, \quad x_2 = X_2 \mathrm{e}^{i\Omega t} \quad (4)$$

represent a trial solution for natural oscillations at frequency Ω at complex amplitudes X_1 and X_2, equations (3) become,

$$-\Omega^2 \mathbf{M}\mathbf{X} + \mathbf{K}\mathbf{X} = \mathbf{0}. \quad (5)$$

Letting $\lambda = \Omega^2$, rearranging terms, and multiplying through by $\mathbf{M}^{-1}$,

$$\mathbf{M}^{-1}\mathbf{K}\mathbf{X} = \mathbf{A}\mathbf{X} = \lambda \mathbf{X}. \quad (6)$$

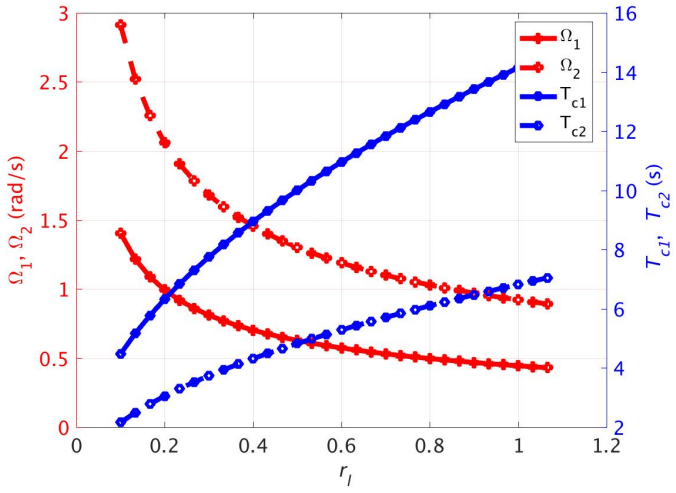

Fig. 2: Dependence of coupled natural frequencies (periods) in heave on tube/water-column length. The second (antisymmetric) mode is more suitable for energy conversion through relative oscillation. For design purposes a desired length-range could generally be identified, depending on the expected region of operation.

Equation (6) represents an eigenvalue problem. The two eigenvalues $\lambda_1 > \lambda_2$ give the two coupled natural frequencies according to,

$$\Omega_1 = \sqrt{\lambda_1}, \quad \text{and} \quad \Omega_2 = \sqrt{\lambda_2}, \tag{7}$$

where the positive square-roots are used. The two eigenvectors $\mathbf{e}_1$ and $\mathbf{e}_2$ represent the two modes of oscillation. The first mode $\mathbf{e}_1$ at Ω_1 comprises in-phase oscillations of the two masses m_1 and m_2, while in the second mode the two masses oscillate with opposite phases. Since the goal here is to utilize the relative oscillations between the collar+tube structure and the water within the tube, the asymmetric mode is of most interest.

Figure 2 plots the coupled natural frequencies and periods for a range of the ratio $r_l = L/L_t$, where L denotes the submerged lengths of the tube and the oscillating water column chamber, and L_t denotes the available length of a large 533mm diameter torpedo tube (here taken to be 7.5m). The added length coefficient in heave at infinite frequency is taken to be 1.5. Also plotted in the figure are the coupled natural periods ($T_{ci} = (2\pi)/\Omega_i,\ i = 1, 2.$).

B. Oscillating Pressure Distribution in a Floating Body

The system being modeled here comprises the tubular buoy with collar and the oscillating water column within the buoy. In the analysis below, the two variables of interest are the collar-tube velocity and the pressure in the air chamber. Heave oscillations are thought to dominate, given the small diameter geometries under consideration here. The device is thought to be equipped with a power take-off that is driven by the oscillating pressurized air flow flux caused by the combined action of the surrounding wave field and the oscillations of the floating buoy. Water oscillation inside the tube is driven by both the surrounding wave field and buoy oscillations, and causes the pressure in the chamber to rise and fall. In turn, the chamber pressure oscillations can cause the water in the tube to oscillate, which simultaneously causes the buoy to oscillate.

The air/water oscillations inside the tube are expressed using flow fluxes (i.e. flow velocity $\times$ tube area). The action of the wave field causes a flow flux through the tube which causes chamber pressure oscillations. The oscillating pressure over the water surface causes its own oscillating flow flux and hence radiates waves. The floating body oscillations effectively cause a flow flux (and hence pressure oscillations) in the tube. This pressure in turn causes a force that can affect buoy oscillations. This coupled dynamic interaction in the time domain is represented using,

$$(m_1 + \overline{a}(\infty))\dot{v}(t) + \int_0^\infty h_r(\tau)v(t-\tau)d\tau + \int_0^t kv(\tau)d\tau - \int_0^\infty s_r(\tau)p(t-\tau)d\tau = f_e(t). \tag{8}$$

where $m_1 = \rho A_{wp} D_r$. h_r is the causal impulse-response function for collar heave (e.g. see [12]), k is the collar stiffness coefficient in heave, s_r is the impulse-response function representing the dynamic coupling between the collar oscillations v and chamber air pressure p. Additionally, for the oscillating pressure distribution within the tube,

$$q_d + q_r + q_c = q_t. \tag{9}$$

where q_d is the diffraction flow rate (assuming the buoy is held fixed in the waves, and the chamber is fully open to atmosphere), q_r is the radiation flow rate due to oscillating chamber pressure, q_c is the flow rate caused by buoy oscillations without waves. The total flow flux q_t drives the power take-off. q_d is frequency dependent and requires solution of the diffraction problem. q_r and q_c are also frequency dependent and require solution of two radiation problems.

To derive some insights into the overall dynamics, this paper focuses on a frequency-domain analysis of the coupled system outlined in equations (8) and (9). Fourier transformation of both sides of equation (8) results in,

$$\left[i\omega\left(m_1 + \overline{a}(\infty) + a(\omega)\right) + \frac{1}{i\omega}k + b(\omega) + c_D\right] v(i\omega) - S(i\omega)P(i\omega) = F_f(i\omega), \tag{10}$$

where $a(\omega)$ is the frequency-dependent added mass in heave for the collar, $b(\omega)$ being the radiation damping, c_D is the linearized viscous friction damping, with $v(i\omega)$ representing the heave-velocity complex amplitude, and $S(i\omega)$ and $P(i\omega)$ denoting the frequency-dependent coupling coefficient and chamber pressure complex-amplitude respectively.

Fourier transforming equation (9),

$$-Q_r(i\omega) - Q_c(i\omega) + Q_t(i\omega) = Q_d(i\omega). \tag{11}$$

Here, the frequency-domain radiation flow flux $Q_r(i\omega) = C(i\omega)P(i\omega)$, $Q_c(i\omega) = S(i\omega)v(i\omega)$, and $Q_t(i\omega) = \Lambda(i\omega)P(i\omega)$, with $C(i\omega)$ denoting the radiation admittance, and $\Lambda(i\omega)$ denotes the complex load applied by the power take-off on the chamber pressure. The complex coefficients can be broken down as,

$$\begin{aligned} C(i\omega) &= B(\omega) + i\omega A(\omega), \\ S(i\omega) &= G(\omega) + i\omega J(\omega), \\ \Lambda(i\omega) &= R(\omega) + i\omega L(\omega). \end{aligned} \tag{12}$$

Here $B(\omega)$ and $A(\omega)$ denote the radiation conductance and susceptance respectively that relate the chamber pressure to the radiation flow-flux responsible for wave generation by the oscillating water column. $G(\omega)$ and $J(\omega)$ are the radiation coupling coefficients that quantify the interaction between the collar+tube structure oscillations and the chamber pressure and vice versa.

The following section describes the method used here to evaluate the hydrodynamic coefficients $b(\omega)$, $a(\omega)$, $B(|omega)$, $A(\omega)$, $J(\omega)$ and $G(\omega)$. The coefficients $R(\omega)$ and $L(\omega)$ are determined by the action of the power take-off system, which is not considered here in order to maintain the generality of this work at this stage.

III. Determining the Hydrodynamic Coefficients

From Figure 2 it is seen that a tube length of $0.6L = 4.5$m gives an asymmetric coupled natural period $T_{c2} \rightarrow 5.0$s, for which the deep-water wavelength is $\approx$ 39.0m. Since the diameters of the collar and tube are much smaller than this and other wavelengths around it (i.e. $kD_c \ll 1$), e.g. for the collar $D_c = 0.533$m, $kD_c = 0.085$) a Froude-Krylov approximation is justified In other words, the near-field effects of diffraction can be neglected, and the quantifies f_e and q_d and their frequency-domain counterparts can be evaluated using the incident-wave elevation alone. As part of this frequency-domain analysis, the wave elevation for a wave traveling from left to right is represented as,

$$\eta_I(x,t) = A\mathrm{e}^{-i(kx-\omega t)} = A\mathrm{e}^{-i(kr\cos\theta-\omega t)}. \tag{13}$$

Given the radial symmetry of the geometry being studied, it is convenient to use a partial-wave expansion to express the spatial part of equation (13) as,

$$\eta_I(r,\theta) = A\sum_{n=0}^{\infty} \varepsilon_n(-i)^n J_n(kr)\cos n\theta. \tag{14}$$

Here A is the wave amplitude, J_n is the Bessel function of the first kind and order n, $\varepsilon = 1$ for $n = 0$, and $\varepsilon = 2$, $n > 0$. Since the collar is axi-symmetric, integration of all terms with $\cos n\theta \rightarrow 0$ for $n > 0$. The heave exciting force F_f can now be found as,

$$\begin{aligned} F_f(i\omega) &= -\rho g A \int_{r_t}^{r_a} rJ_0(kr)dr \int_0^{2\pi} d\theta \\ &= -\frac{2\pi\rho a A}{k}\left(r_a J_1(kr_a) - (r_t J_1(kr_t)\right). \end{aligned} \tag{15}$$

The diffraction flow flux under the Froude-Krylov approximation can be found using,

$$\begin{aligned} Q_d(i\omega) =& A\int_0^{r_t}\int_0^{2\pi} r\omega\eta_I dr d\theta = A\int_0^{r_t}\int_0^{2\pi} r\omega J_0(kr)drd\theta, \\ =& \frac{2\pi A\omega}{k} r_t J_1(kr_t). \end{aligned} \tag{16}$$

It is noted that both F_f and Q_d are real-valued. Using Haskind relations for a radially symmetric body (e.g. [13]), the radiation damping coefficient $b(\omega)$ for the collar can be found as,

$$b(\omega) = \frac{k}{8P_w}|F_f(i\omega)|^2;\ P_w = \frac{\rho g^2 A^2}{4\omega}. \tag{17}$$

P_w is the incident wave power per unit crest length. Similarly, the radiation conductance $B\omega)$ for the oscillating pressure distribution in the chamber can be found using,

$$B(\omega) = \frac{k}{8P_w}|Q_d(i\omega)|^2. \tag{18}$$

The radiation coupling term $J(\omega)$ can be found using [11],

$$-iJ(\omega) = \frac{k}{8P_w} Q_d(i\omega)F_d^*(i\omega). \tag{19}$$

The coefficients $a(\omega)$, $A(\omega)$, and $G(\omega)$ can be determined using the Kramer's-Kronig relationships and direct evaluation of the principal value integrals below. Thus,

$$a(\omega) = \frac{2}{\pi}\ \mathrm{PV}\int_0^{\infty} \frac{b(\varpi)}{\varpi^2-\omega^2}d\varpi. \tag{20}$$

Here ω denotes the frequency at which $a(\omega)$ is to be evaluated, while ϖ is the frequency variable for integration. Next,

$$A(\omega) = \frac{2}{\pi}\ \mathrm{PV}\int_0^{\infty} \frac{B(\varpi)}{\varpi^2-\omega^2}d\varpi. \tag{21}$$

Finally,

$$G(\omega) = \frac{2}{\pi}\ \mathrm{PV}\int_0^{\infty} \frac{\varpi^2 J(\varpi)}{\varpi^2-\omega^2}d\varpi. \tag{22}$$

It is relatively straightforward to evaluate all of the the hydrodynamic quantities (including exciting force, and diffraction flow flux) using a computing environment such as Matlab. Results of these calculations are reported in this paper.

IV. Discussion of Results

Our work so far suggests that there are significant opportunities to optimize the natural response of the torpedo-tube deployable free-floating wave energy devices, so that they can provide the expected power outputs in a range of wave climates and deployment sites. Our design emphasis is on providing the desired performance without active control, essentially allowing the devices to perform with little intervention for long periods of time. The asymmetric mode with natural frequency Ω_{c2} (natural period T_{c2}) is more suitable for power conversion.

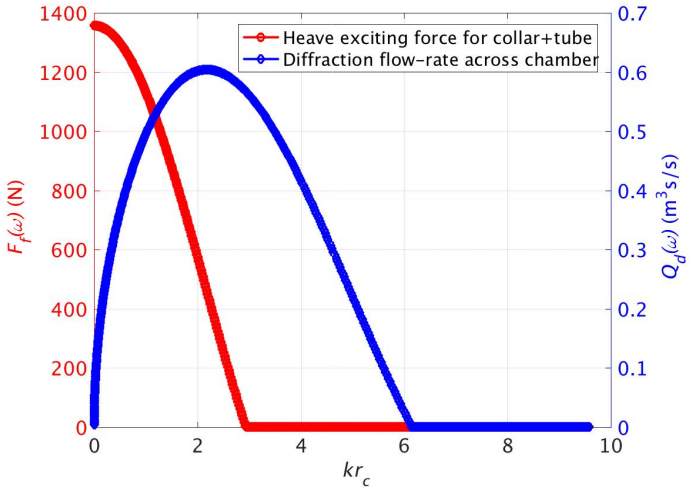

Fig. 3: Wave-applied exciting force in heave on the collar-tube structure and the diffraction flow rate through the oscillating water column tube.

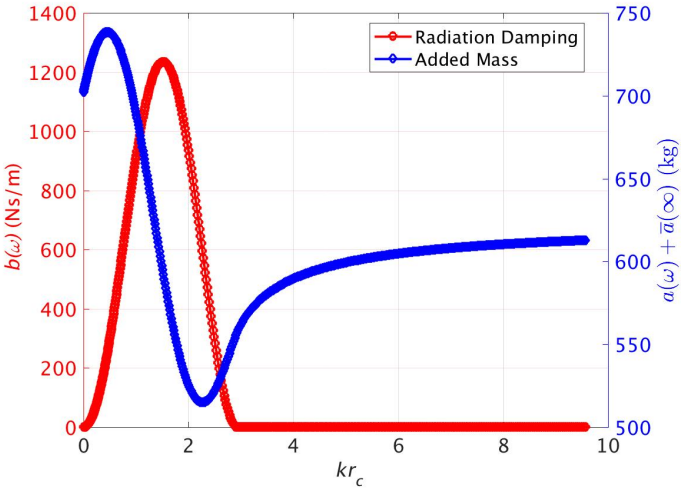

Fig. 4: Radiation damping and added mass for the collar-tube structure. The infinite-frequency added mass in heave is taken to be equal to the in-air mass of the collar-tube structure.

Results for the hydrodynamic coefficients and the forcing terms as evaluated using equations (15)–(22) are discussed below. These results are plotted as functions of the non-dimensionalized wave number kr_c, where r_c is the radius of the collar. Figure 3 plots the exciting force in heave for the collar-tube structure and the diffraction flow flux through the oscillating water column. The maximum value for the exciting force is seen to be roughly 1360N, and it occurs, as expected at zero kr_c (i.e. zero frequency), given that the Froude-Krylov term dominates the diffraction part at low frequencies, and that the present treatment uses the Froude-Krylov approximation to determine all of the hydrodynamic quantities discussed here. The diffraction flow rate reaches a maximum value of 0.6 m^3/s at $kr_c \sim 2.2$. This value of kr_c is somewhat large for most wave conditions from which energy is to be converted, At a period of 5s, on the other hand, $F_f \sim 1350$N, while $Q_d = 0.1644$ m^3/s, which give an idea of the approximate magnitudes that the device may experience in wind-sea dominated wave conditions.

The radiation damping and added mass in heave of the collar-tube structure are plotted in Figure 4. It can be seen that the radiation damping reaches a maximum of about 1230 Ns/m at $kr_c \sim 1.5$, while the added mass varies between about 510 and 740 kg. The infinite-frequency added mass in heave is taken to be equal to the in-air mass of the collar-tube structure. Close to an expected operating period of 5s, the radiation damping constant is about 20 Ns/m while the added mass is about 710 kg. The relatively small radiation damping value implies potentially large oscillation amplitudes if resonance occurs close to 5s.

The hydrodynamic coefficients for the oscillating pressure in the air chamber within the tube are shown in Figure 5. The conductance reaches a maximum value of about 2.2×10^{-3} m^{4}s/kg near kr_c of about 3.5, while the susceptance varies

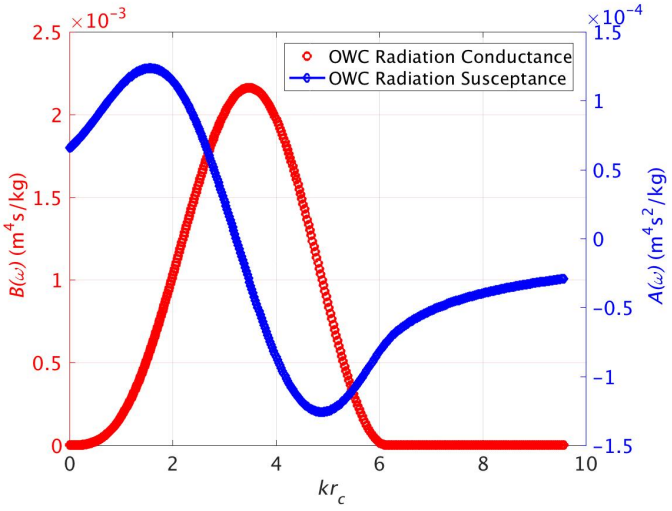

Fig. 5: Conductance and susceptance for the oscillating pressure within the tube, as computed using the procedure in section III.

between roughly $\pm 1.2 \times 10^{-4}$ m^{4}s^2/kg. Close to a wave period of 5s, the conductance is approximately 1.9×10^{-5} and susceptance is about 8.3×10^{-5}. It would be potentially interesting to study how changes in the device geometry might influence these quantities, so that operation close to an optimum variable range for the power take-off mechanism is possible.

The radiation coupling coefficients (i,e. effect of the oscillating pressure within the air chamber on the heave oscillations of the collar-tube structure and vice versa) are plotted in Figure 6. The overall behavior is similar to that observed for the collar-tube and oscillating pressure coefficients. The real part $J(\omega)$

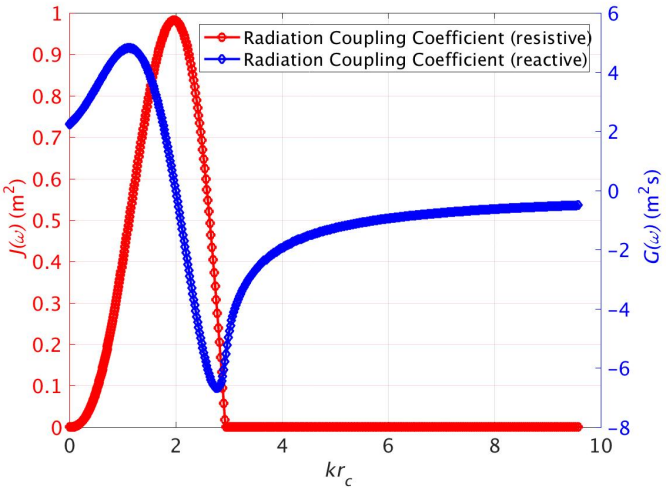

Fig. 6: Radiation coupling coefficients (i.e. real and imaginary parts of the complex radiation coupling coefficients, as defined in section II-B and computed using the procedure in section III.

reaches a maximum of about 1.0 m^2 near $kr_c \sim 2.0$, while the imaginary part $G(\omega)$ varies between -7 and 5 m^{2}s over the wave number range considered here. On the other hand, close to a wave period of 5s, the real part $J(\omega)$ is about 1.7×10^{-3} m^2, while the imaginary part $G(\omega)$ is about 2.4 m^{2}s. Overall, the coefficient ranges estimated here suggest an interesting dynamic behavior which would be important to investigate using both frequency and time domain models.

V. Concluding Remarks

A tubular device capable of fitting within large torpedo tubes was considered in this paper. The device utilizes an oscillating water column type primary converter. A coupled dynamic model based on the theory of oscillating pressure distributions within floating bodies was used to derive the hydrodynamic coefficients and forcing terms needed. An approximate two-degree of freedom rigid-body model was first used to help determine design parameters for the device. Immediate next steps include frequency-domain solutions that provide an assessment of the dynamic response and power conversion characteristics of the device in a range of wave climates. Time-domain simulations are also planned for chosen irregular wave conditions, in part to incorporate more realistic power take-off models. Several important design tasks (e.g. buoyancy and mass distributions for self-righting, dynamic stability, freeboard minimization, etc.) need to be completed before these devices can be considered fully mission-capable.

References

[1] A. LiVecchi, A. Copping, D. Jenne, A. Gorton, R. Preus, G. Gill, R. Robichaud, R. Green, S. Geerlofs, S. Gore *et al.*, "Powering the blue economy; exploring opportunities for marine renewable energy in maritime markets," *US Department of Energy, Office of Energy Efficiency and Renewable Energy. Washington, DC*, p. 207, 2019.

[2] R. Green, A. Copping, R. J. Cavagnaro, D. Rose, D. Overhus, and D. Jenne, "Enabling power at sea: Opportunities for expanded ocean observations through marine renewable energy integration," in *OCEANS 2019 MTS/IEEE SEATTLE*. Seattle, WA, USA: IEEE, October 2019, pp. 1–7. [Online]. Available: https://ieeexplore.ieee.org/document/8962706

[3] B. P. Driscol, L. A. Gish, and R. G. Coe, "A scoping study to determine the location-specific wec threshold size for wave-powered auv recharging," *IEEE Journal of Oceanic Engineering*, pp. 1–10, 2020. [Online]. Available: https://ieeexplore.ieee.org/document/9044418

[4] M. E. McCormick, *Ocean Wave Energy Conversion*. John Wiley and Sons, NY, 1981, reissued with revisions by Dover Inc, NY in 2007.

[5] K. Budal and J. Falnes, "Wave power conversion by point absorbers," *Norwegian Maritime Research*, vol. 6, no. 4, pp. 2–11, 1978.

[6] T. Whittaker, F. McPeake, and A. Barr, "The development and testing of a wave-activated navigational buoy with a Wells Turbine," *Journal of Energy Resources Technology*, vol. 107, no. 2, pp. 268–273, 1985.

[7] U. A. Korde, "Latching control of deep water wave energy devices using an active reference," *Ocean Engineering*, vol. 29, pp. 1343–1355, 2002.

[8] R. Gomes, J. Henriques, L. Gato, and A. Falco, "Hydrodynamic optimization of an axisymmetric floating oscillating water column for wave energy conversion," *Renewable Energy*, vol. 44, pp. 328–339, 2012. [Online]. Available: https://www.sciencedirect.com/science/article/pii/S0960148112001413

[9] A. O. Falco and P. Justino, "Owc wave energy devices with air flow control," *Ocean Engineering*, vol. 26, no. 12, pp. 1275–1295, 1999. [Online]. Available: https://www.sciencedirect.com/science/article/pii/S0029801898000754

[10] D. V. Evans, "Wave power absorption by systems of oscillating surface pressure distributions," *Journal of Fluid Mechanics*, vol. 114, pp. 481–499, 1 1982.

[11] J. Falnes and P. McIver, "Surface wave interactions with systems of oscillating bodies and pressure distributions," *Applied Ocean Research*, vol. 7, no. 4, pp. 225–234, 1985.

[12] W. Cummins, "The impulse response function and ship motions," David Taylor Model Basin DTNSRDC, Tech. Rep., 1962.

[13] J. N. Newman, *Marine Hydrodynamics*. Cambridge: MIT Press, 1978, second Printing, Call No. (VM 156.N48)., ix + 402 pp.